Martin Marietta Laboratories

MARTIN MARIETTA

MML TR 90-28c

A STUDY OF THE INFLUENCE OF ALLOYING ADDITIONS ON THE PASSIVITY OF ALUMINUM

Annual Report
Period:

December 1, 1988 - November 30, 1989

Prepared for:
Office of Naval Research
800 North Quincy Street
Arlington, Virginia 22217-5000

Submitted By:
B.A. Shaw, G.D. Davis, T.L. Fritz

Martin Marietta Laboratories
1450 South Rolling Road
Baltimore, Maryland 21227-3898

and

W.C. Moshier
Martin Marietta Space Systems
Denver, Colorado 80201

February 1990

MML TR 90-28c

A STUDY OF THE INFLUENCE OF ALLOYING ADDITIONS ON THE PASSIVITY OF ALUMINUM

Annual Report
Period:

December 1, 1988 - November 30, 1989

Prepared for:
Office of Naval Research
800 North Quincy Street
Arlington, Virginia 22217-5000

Submitted By:
B.A. Shaw, G.D. Davis, T.L. Fritz

Martin Marietta Laboratories
1450 South Rolling Road
Baltimore, Maryland 21227-3898

and

W.C. Moshier
Martin Marietta Space Systems
Denver, Colorado 80201

February 1990

Unclassified
SECURITY CLASSIFICATION OF THIS PAGE

REPORT DOCUMENTATION PAGE

1a REPORT SECURITY CLASSIFICATION Unclassified	1b RESTRICTIVE MARKINGS None
2a SECURITY CLASSIFICATION AUTHORITY	3 DISTRIBUTION AVAILABILITY OF REPORT Unlimited
2b DECLASSIFICATION / DOWNGRADING SCHEDULE None	
4 PERFORMING ORGANIZATION REPORT NUMBER(S) MML TR 90-28c	5 MONITORING ORGANIZATION REPORT NUMBER(S)
6a NAME OF PERFORMING ORGANIZATION Martin Marietta Corporation Martin Marietta Laboratories 6b OFFICE SYMBOL (If applicable) MML	7a NAME OF MONITORING ORGANIZATION Defense Contract Administration Services Management Area- Baltimore
6c ADDRESS (City, State, and ZIP Code) 1450 South Rolling Road Baltimore, Maryland 21227-3898	7b ADDRESS (City, State, and ZIP Code) 300 East Joppa Road Baltimore, Maryland 21204-3099
8a NAME OF FUNDING SPONSORING ORGANIZATION Office of Naval Research 8b OFFICE SYMBOL (If applicable) ONR	9 PROCUREMENT INSTRUMENT IDENTIFICATION NUMBER N00014-85-C-0638
8c ADDRESS (City, State, and ZIP Code) 800 North Quincy Street Arlington, VA 22217-5000	10 SOURCE OF FUNDING NUMBERS PROGRAM ELEMENT NO / PROJECT NO / TASK NO / WORK UNIT ACCESSION NO

11 TITLE (Include Security Classification) A Study of the Influence of Alloying Additions on the Passivity of Aluminum

12 PERSONAL AUTHOR(S) B.A. Shaw, G.D. Davis, T.L. Fritz and W.C. Moshier

13a TYPE OF REPORT Annual	13b TIME COVERED FROM 12/1/88 TO 11/30/89	14 DATE OF REPORT (Year, Month, Day) February 1990	15 PAGE COUNT

16 SUPPLEMENTARY NOTATION

17 COSATI CODES		
FIELD	GROUP	SUB-GROUP

18 SUBJECT TERMS (Continue on reverse if necessary and identify by block number)
Approved for public release; distribution unlimited. Reproduction in whole or in part is permitted for any purpose of the United States Government.

19 ABSTRACT (Continue on reverse if necessary and identify by block number)

The susceptibility of aluminum and aluminum alloys to pitting in aqueous chloride-containing environments is well known. Typical aluminum alloying constituents such as copper, silicon, zinc, and magnesium are added to improve mechanical properties, and not to provide corrosion resistance. Passivity-enhancing species, such as Cr, Mo, Ta and W, typically exhibit very low solubility limits in aluminum, well below 1 at.%, and at these concentrations exert little influence on corrosion behavior. The solubility limits for these elements in aluminum can be exceeded and corrosion performance enhanced if the alloys are produced using a rapid solidification method such as vapor deposition. In this fourth year of the program the corrosion resistance of three binary alloys Al-V, Al-Nb, and Al-W and one physically vapor deposited ternary alloy are evaluated. The Al-W alloys exhibit the best localized corrosion resistance observed to date with increases in E_p up to 2600 mV with the addition of 10.3at.% W to Al. Additionally, the corrosion performance of Al-8at.% W specimens that were heat treated to produce a two-phase alloy are comparable to those found earlier for

20 DISTRIBUTION / AVAILABILITY OF ABSTRACT ☐ UNCLASSIFIED/UNLIMITED ☐ SAME AS RPT ☐ DTIC USERS	21 ABSTRACT SECURITY CLASSIFICATION Unclassified
22a NAME OF RESPONSIBLE INDIVIDUAL Dr. Guy D. Davis	22b TELEPHONE (Include Area Code) 301-247-0700 ext 2376

DD FORM 1473, 84 MAR 83 APR edition may be used until exhausted
All other editions are obsolete

SECURITY CLASSIFICATION OF THIS PAGE

☆ U.S. Government Printing Office: 1985-544

ABSTRACT

The susceptibility of aluminum and aluminum alloys to pitting in aqueous chloride-containing environments is well known. Typical aluminum alloying constituents such as copper, silicon, zinc, and magnesium are added to improve mechanical properties and not to provide corrosion resistance. Passivity-enhancing species, such as Cr, Mo, Ta and W, typically exhibit very low solubility limits in aluminum, well below 1 at.%, and at these concentrations exert little influence on corrosion behavior. The solubility limits for these elements in aluminum can be exceeded and corrosion performance enhanced if the alloys are produced using a rapid solidification method such as vapor deposition. In this fourth year of the program the corrosion resistance of three binary alloys Al-V, Al-Nb and Al-W and one physically vapor deposited ternary alloy are evaluated. The Al-W alloys exhibit the best localized corrosion resistance observed to date with increases in E_p up to 2600 mV with the addition of 10.3at.% W to Al. Additionally, the corrosion performance of Al-8at.% W specimens that were heat treated to produce a two-phase alloy are comparable to those found earlier for single-phase Al-8at.% Mo alloys. Characterization of the physically vapor deposited ternary alloy reveals that several atomic percent of passivity enhancing species can be retained in solid solution with this process and therefore this technique is very promising for the production of nonequilibrium corrosion-resistant aluminum alloys.

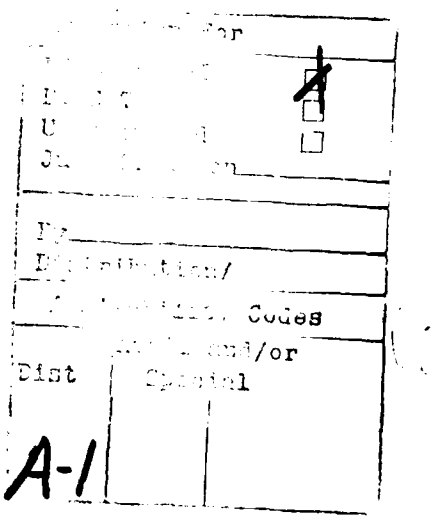

1.0 INTRODUCTION

Many of the alloying additions responsible for the corrosion resistance of stainless steels can also be used to enhance the passivity of aluminum, provided that these elements remain in solid solution in the alloy. However, passivity-enhancing elements such as Cr, Mo, Ta, Zr, and W typically exhibit very low solubility limits in aluminum, below 1at.%, and at these concentrations exert little influence on corrosion behavior. The amount of solute in solution can be increased above the solubility limit with a concomitant enhancement in corrosion performance if the alloys are produced by rapid solidification. Two processes capable of producing aluminum solid solutions with solute concentrations on the order of 5 to 10at.% are sputter deposition and vapor deposition. Sputter deposition is limited to thin film applications, whereas vapor deposition is currently being used in the United Kingdom for the production of Al-Cr-Fe sheet material.

Previously (1-6), we have investigated the roles that Cr, Mo, Zr, Cu, Si and Ta play in altering the protective nature of aluminum passive films using potentiodynamic polarization and X-ray photoelectron spectroscopy (XPS). The most significant enhancements in the localized corrosion resistance of these thin film alloys were observed for the Al-Cr, Al-Ta and Al-Mo alloys. In aerated 0.1 M KCl, Al-4at.% Cr alloys exhibited an average shift in E_p, the pitting potential, of 600 mV; Al-6at.% Ta alloys exhibited an average shift of 750 mV, and Al-8at.% Mo alloys exhibited an average shift in E_p of 800 mV. Surface analysis of the passive films formed on these alloys revealed that they become enriched in oxidized solute as the specimen is anodically polarized. In general, the oxidized solute protects the substrate by restricting the ingress of chloride and thereby preventing localized attack.

In this fourth year of the program we have added Nb, V, and W to the list of alloying additions investigated and we have also examined an Al-Cr-Fe vapor-deposited bulk material. Of the three alloying additions evaluated this year, tungsten is of particular interest since, like Ta, it is known to be very resistant to localized corrosion (7) and because its addition to stainless steels has resulted in significant improvements in the localized corrosion resistance (8) of these alloys.

2.0 EXPERIMENTAL PROCEDURE

2.1 Specimen Preparation

The alloy films were produced by RF magnetron sputter deposition onto single-crystal Si wafers with a 2-in. diameter (5.08 cm). All of the films, except the low-W concentration Al-W films, were deposited to a thickness of 200 nm using a cosputter deposition process, which is described in detail elsewhere (1-6,9). Briefly, this process involves using two target materials, and sputtering the solute at a low power level, typically 15 to 40 watts, and the Al at a higher power of approximately 360 watts. The cosputter deposition process produces a gradient in solute concentration across the 2-in. wafers, with low solute concentrations on the side of the wafer closest to the Al target, and higher concentrations on the side closest to the solute target. Cosputter deposition allows us to evaluate a range of compositions, that typically differ by several atomic percent across the wafer, without having to produce numerous individual wafers.* The low-W concentration Al-W alloys were sputtered using two identical alloyed targets (Al-1%W) and were deposited to a thickness of 1 to 2 μm. This process allows much finer control of alloy composition over the surface of the wafer. These films were deposited to greater thicknesses because of some problems getting continuous coverage of the Si wafer with the thinner films. For both the sputter-deposited and the cosputter-deposited films the substrates were kept at 77 K to discourage precipitate formation during the deposition process and to produce fine-grained structures. Solute concentrations for all of the alloys were determined by induction-coupled plasma (ICP); XPS was used to nondestructively determine concentrations on individual Al-W specimens cleaved from the 2-in. wafers. All references to solute concentration in the text of this report are values determined by XPS, unless otherwise noted.

The Al-Cr-Fe bulk material was obtained from the Royal Aerospace Establishment (RAE) in the United Kingdom where it is produced under the designation RAE alloy 72. The chemical composition for the 1.6-mm sheet product that we evaluated is given in Table 1. The vapor deposition process used to produce the sheet, described generically in several publications (10,11,12), involves the electron beam evaporation of alloyed targets and then condensation from the

---

* All concentrations are in atomic percent unless otherwise noted.

vapor phase onto controlled temperature collectors. The deposit is mechanically worked during the deposition and then rolled to a final thickness of a few millimeters.

TABLE 1

Chemical Composition of RAE 72 Sheet

Element	Concentration (at.%)
Cr	4.32
Fe	0.56
Al	Balance

2.2 Electron Microscopy and X-ray Diffraction

High resolution scanning electron microscopy (HSEM) of the as-sputtered surfaces was performed on a JEOL 100 CX at 40 keV. The specimens were evaluated in the as-deposited condition, (i.e., without a thin coating of C or Pt sputtered on top of the alloy film) to ascertain grain morphology and size.

Glancing incident X-ray diffraction (GXRD) (13), with a constant angle of 10 degrees between the incident X-ray beam and the film surface, was used to check each of the alloys for precipitate formation shortly after production and after long-term storage. The experiments were performed on a Scintag diffractometer using a monochromatic Cu Kα X-ray source. The glancing angle was chosen both to optimize the signal from the metal film and to prevent diffraction from the Si single crystal substrate.

Several of the Al-W specimens were vacuum encapsulated in quartz and heat treated at 400°C for 1 hour to drive precipitate formation. The concentrations of W in these films were between 8.1 and 8.2%. Following this heat treatment, GXRD was used to check for the presence of precipitates. The localized corrosion resistance of these specimens was also evaluated using potentiodynamic polarization.

2.3 Electrochemical Measurements

Individual electrochemical specimens were prepared by cleaving the Si single-crystal wafers into 0.5- x 0.5-cm pieces, attaching a coated lead wire, and masking the back and edges of the specimens with a two-part marine epoxy paint (Interlux 404). Anodic potentiodynamic polarization curves were generated at a scan rate of 0.2 mV/s at ambient room temperatures (23 to 27°C). A limited number of experiments were also run at scan rates of 0.08 and 0.05 mV/s to determine if the scan rate was effecting E_p. The RAE alloy specimens were then polished with 500 grit; cleaned ultrasonically in acetone, methanol, and distilled, deionized water; rinsed in distilled, deionized water; and blown dry with nitrogen. They were then mounted and masked identically to the sputter-deposited specimens.

With the vapor-deposited bulk alloy, we also used an "electrochemical scratch" technique, also known as the "pitting propagation rate method" (14,15) or the "quasi-stationary anodic polarization method for determining the repassivation potential" (16), to determine the repassivation or protection potential. This technique is identical in principle to Pessal and Liu's scratch technique, but employs an instantaneous, high-voltage pulse (on the order of 1 to 2 V) to momentarily breakdown the passive film instead of an actual scratch on the specimen surface. After the passive film has been broken down, the potential is quickly returned to a set value within the passive region, and the current is monitored for several minutes. This process is initiated at the open circuit potential, E_{oc}, and then repeated at increasingly positive potentials until the current no longer decreases after the voltage pulse. This critical potential is the repassivation or protection potential, not the pitting potential, although many believe that the two are synonymous for Al. It was not possible to use this technique on the alloy films because once pitting is initiated on such thin films, the Si substrate is exposed. All of the electrochemical experiments were conducted on at least duplicate specimens. Most of the experiments were conducted in deaerated 0.1 M KCl at a pH of 7; however, some were conducted in deaerated 0.1 M KCl at a pH of 8. After immersion and prior to testing, the open circuit potentials were allowed to come to steady state, and generally stabilized within 1 hour. All potentials given in this report are versus a saturated calomel electrode (SCE).

2.4 Surface Analysis

The chemistry of the Al-W passive film was investigated in the as-deposited condition at E_{oc} and at potentials up to E_p. Details of the procedure have been reported previously (2,4). The polarization experiments were conducted in aerated 0.1 M KCl at a pH of 7. Changes in the surface chemistry induced by the transfer procedure and by exposure to ultrahigh vacuum have been examined in detail (4,17,18). Possible experimental artifacts were shown to be either small, (e.g., additional oxidation) or tractable (e.g., adventitious contamination), and measured differences in surface chemistry were shown to occur in the electrolyte.

The XPS measurements were made using a Surface Science Instruments Model SSX 100-03 spectrometer with a monochromatized Al Kα X-ray source and a hemispherical electron energy analyzer with multichannel detection. The X-ray source was focused to a spot size of 600 μm, and the surface charge was neutralized with low-energy electrons. Binding energies were normalized to that of adventitious hydrocarbon at 284.6 eV. Survey spectra provided a qualitative analysis of the surface, whereas high-resolution spectra [with a full width at half maximum (FWHM) of the Au $4f_{7/2}$ peak of 1.1 eV] of the O 1s, C 1s, Al 2p, and W 4f photoelectron peaks were used for quantitative analysis and chemical state determination. Quantitative analysis was obtained using peak areas and sensitivity factors determined from standards with our spectrometer. Chemical state separation was achieved by curve fitting, the details of which are presented in Ref. (4).

2.5 Salt Fog Testing

Salt fog exposures were conducted on duplicate specimens to establish the resistance of the alloys to attack in this type of environment. The tests were conducted in accordance with ASTM B117-85 "Standard Method of Salt Spray (Fog) Testing" (19) using a Singleton model 20 corrosion cabinet. The tests were conducted at a temperature of 35°C. A 5wt% NaCl solution was used to produce the fog. The degree of attack was determined visually; hence, they are qualitative evaluations.

3.0 RESULTS

3.1 Alloy Characterization

Chemical analysis of the Al-Nb and Al-V alloy specimens revealed the expected gradient in solute concentration across the wafers, with high solute concentrations on one side of the wafer and low concentrations on the other side. Similar gradients have been observed for the alloys evaluated in previous years. The range in solute concentrations observed for the Al-V and Al-Nb films deposited at power settings of 40 watts for the solute target and 360 watts for the Al target are presented in Table 1. Although the power applied to the Al targets to produce each of the thin alloy specimens was the same, the solute concentrations vary considerably. The solute concentration as a function of distance across the wafer for the cosputter-deposited Al-W wafers were not as clear. The cosputter-deposited Al-W alloys tended to have higher solute concentrations on one side of the wafer and lower concentrations on the other. However, a linear gradient in concentration from one side of the wafer to the other was not observed. Analysis of localized areas within a 0.5- x 0.5-cm section removed from the 2-in. wafer revealed W variations of several atomic percent between areas a few millimeters apart. No noticeable pattern for the W concentration with respect to target orientation could be established. The lack of a consistent linear concentration gradient in the Al-W cosputter-deposited alloys is puzzling and at present we do not have an explanation for why the sputtering characteristics of W are unlike that of the other materials we have investigated. One way we have found to circumvent this problem is to use binary targets for the production of the Al-W thin-film alloys. Solute concentration data, including bulk analysis of 0.5- x 0.5-cm sections by ICP and localized analyses of 600-μm x 900-μm areas by XPS, are presented in Table 2.

The Al-W specimens produced from the Al-1at.% W binary targets exhibited uniform W concentrations from point to point on the wafer, and as expected, no gradient in W concentration was observed. The ranges in composition observed for these alloys are presented in Table 3. Note that the W concentration is higher in the specimen than in the target. This difference may be due to resputtering of deposited Al atoms from the specimen or differences in the sticking coefficients of the two elements.

TABLE 2

Variation in Solute Concentration Across
Cosputter Deposited Alloy Films
(on 2-in.-dia. wafers)

Alloy Designation	Concentration (at.%)			
	ICP		XPS	
	Low	High	Low	High
Al-Nb	4.8	9.6	--	--
Al-V	0.7	2.6	--	--
Al-W1	3.1	6.9	--	--
Al-W2	2.0	12.8	7.0	11.6
Al-W3	1.2	8.5	--	--
Al-W4	5.5*		6.3	11.3
Al-W5	4.3*		7.9	11.0
Al-W6	4.7	10.8	--	--
Al-W7	2.0	5.6	7.1	11.2
Al-W8	1.6	6.1	5.7	11.9
Al-W9	1.5	5.9	7.5	12.3

* Analysis of specimens removed from center of the wafer.

TABLE 3

Variation in Solute Concentration for Al-W Sputter-Deposited Thin Films Produced from Al-W Binary Targets

Alloy Designation	Concentration ICP (at.%)	
	High	Low
Al-1W1	1.5	1.6
Al-1W2	1.5	1.6

The surfaces of the alloy films were optically reflective and examination using HSEM showed the same nodule-like structure that was previously observed for the other alloys. Whereas the average grain size at the surface for the Al-5%Mo and the Al-6%Ta films was on the order of 0.12 μm, TEM of the Al-W films revealed even finer grain sizes on the order of 30 nm.

The alloys were characterized using GXRD shortly after deposition as a function of time over several months to determine their metallurgical stability. With the exception of several of the higher concentration Al-W alloys, the alloys exhibit a highly oriented microstructure, with only the {111} planes diffracting the beam. A comparison of the GXRD pattern for one of these alloys, Al-8.6%W, with the pattern for sputter-deposited pure aluminum is presented in Fig. 1. We found no evidence of intermetallic phase formation in any of the as-deposited films; the W, Nb, or V was in solid solution with the aluminum and remained in this state during storage at room temperature. The structures of these alloys, like all of the alloys examined to date except the Al-Cu alloys, appear to be stable at room temperature over time, since GXRD after 1 year showed no evidence of precipitates. Precipitates were, however, noted for the Al-W specimens heat treated for 1 h at 400°C. Glancing angle X-ray diffraction of several of the higher W concentration specimens (8.5 to 12.3%) showed no reflections, suggesting that these alloys were amorphous. Selected area diffraction confirmed that these alloys were amorphous. Similar results have been reported for high concentrations of other transition metals in aluminum (20).

The X-ray diffraction pattern for the vapor-deposited Al-Cr-Fe alloy (Fig. 2) also showed only aluminum reflections. Earlier work at RAE (11) documented the presence of a uniform dispersion of very small (3-nm) iron-rich metastable precipitates (p-phase) in this alloy. The absence of these reflections in our X-ray data is attributed to the small size of these precipitates.

3.2 Salt Spray Test

The Al-W alloys and the vapor-deposited Al-Cr-Fe alloy showed the best performance in salt fog tests. After 24 hours of salt fog exposure, one of the pure aluminum specimens, one of the Al-5%Nb (concentration determined by ICP) specimens and both of the Al-2.6%V (concentration determined by ICP) specimens exhibited pitting. After 2 days of exposure, the second pure Al specimen had corroded completely leaving only the bare Si substrate behind. Pits were also observed on the second Al-Nb specimen and small cloudy areas (with no pitting) were noted on both of the Al-1.5%W (concentration determined by ICP) specimens after 2 days. At 5 days, the cloudy areas on the Al-1.5%W specimens had spread and some pits were observed on one of the Al-8.5%W specimens. The second Al-8.5%W specimen retained its mirror finish until the test was terminated at 37 days. The early failure of one of the Al-9%W specimens is believed to have been cause by damage to the film while it was being prepared for exposure in the cabinet. The 200-nm films are very fragile and can be easily damaged when the wafer is cleaved into smaller pieces and when the specimens are mounted and sealed for electrochemical and salt fog tests. The performance of the Al-Cr-Fe specimens were evaluated under identical conditions at a later date and showed no pitting or degradation of the specimen surfaces after 11 days. This test was terminated earlier than the other experiments because of an equipment malfunction.

3.3 Anodic Potentiodynamic Polarization Experiments

Sputter-deposited Al-Cr, Al-Ta, and Al-Mo alloys

Potentiodynamic polarization scans were conducted on Al-Ta, Al-Cr, and Al-Mo specimens at a variety of solute concentrations to determine the role that solute concentration plays in enhancing localized corrosion resistance and to establish minimum solute concentrations that will be need for the bulk alloys to be produced in future years. Solute concentrations for these alloys were determined by ICP. Figure 3 presents the results for Al-Mo and Al-Cr in deaerated 0.1 M KCl. At the lower solute concentrations, the slope of the Al-Cr curve is steeper than the slope of the Al-Mo curve. However, at higher Cr concentrations the slope of the Al-Cr curve flattens out, but the Al-Mo curve continues to increase. Superimposed on these two curves are data points for experiments carried out in aerated 0.1 M KCl. Aeration was found to have little effect on the breakdown potential observed for Al-Cr, but did have an effect on the Al-Mo specimens. Figure 4 shows E_p as a function of solute concentration for Al-Ta alloys in aerated 0.1 M KCl. At the concentrations investigated, E_p appears to exhibit a linear dependence on solute concentration. The slope of the curve is approximately 250 mV/percent of solute and is not quite as steep as the slope observed for the low Cr alloys.

The E_p versus concentration curve for Al-Cr reveals that the addition of 1at.% significantly effects E_p, but that further increases in concentration afford little additional enhancement in corrosion performance. E_p exhibited a stronger dependence on concentration for the Al-Mo and Al-Ta alloys. Of these two alloys, a much steeper concentration slope was observed for the Al-Ta alloys. Based on the Al-W data obtained from the specimens prepared using binary targets (specimens for which we had good control of W concentration) a very steep slope, approximately 550 mV/percent of solute, is anticipated for the E_p versus solute concentration curves for the Al-W alloys. Additional data points, obtained from specimens prepared with binary targets with higher W concentrations, will be need to confirm this slope.

Sputter-deposited Al-Nb and Al-V

The polarization data for two Al-Nb specimens with approximately the same Nb concentrations (4.5 to 5.5% - determined by ICP) are presented in Fig. 5. Both curves exhibit identical passive current densities of approximately 1.5 $\mu A/cm^2$ and similar values for E_p. The 50 mV difference in E_p between the two specimens is attributed to variation in Nb content for the two specimens. Polarization data for two Al-V alloys (0.7 and 1.2%) are presented in Fig. 6. Again, both curves showed similar passive current densities of approximately 1.5 $\mu A/cm^2$, however in this case the breakdown potentials were significantly lower than those of the Al-Nb alloys. A difference in E_p of 70 mV was noted for the two specimens and is, again, attributed to the small variations in solute concentration from specimen to specimen. Figure 7 compares the performance for both of these alloys (average curves) with that reported earlier for Al-8%Mo, Al-4%Cr, Al-8%Ta, Al-3%Zr, and pure Al. (Again, all of the alloys were deposited at the same power level, 360W for the Al target and 40W for the solute target; however, the resultant solute concentration may vary considerably.) This figure reveals that the localized corrosion resistance for the Al-Nb was similar to that observed for Al-Cr and the localized corrosion resistance of the Al-V was similar to that reported for Al-Zr.

Sputter-deposited Al-W

Potentiodynamic polarization scans were generated on 23 specimens taken from various regions of the 9 cosputter deposited Al-W films. All of the specimens exhibited similar open circuit potentials ranging from a low of -700 mV to a high of -584 mV with an average E_{oc} of -653 mV. Earlier it was shown that Mo alloying additions shift the open circuit potential for Al positively, and it was hypothesized that this positive shift was a result of the Mo increasing the exchange current density for the hydrogen reduction reaction. Alloying additions of W also shift the open circuit potential for Al in the positive direction (in both deaerated and aerated solutions) and we, again, attribute this positive shift to an increase in the exchange current density for the reduction reactions as a result of the presence of W in the alloy. The specimens exhibited low passive current densities varying from 1 to 5 $\mu A/cm^2$ and the current densities were found to be independent of potential within the passive region. Since

the solute concentrations for the cosputter deposited films varied considerably from point to point on the films it was not possible to quantitatively establish the relationship between solute concentration and E_p. However, it was observed that specimens with the lowest average solute concentrations (i.e., 1 to 3%) exhibited the lowest breakdown potentials (i.e., -33 to -156 mV). The highest breakdown potentials were observed for specimens with average W concentrations between 6 and 12%. It was interesting to note that pitting potentials for the amorphous alloys (598 mV for an Al-8.5%W alloy and 531 mV for an Al-11.2%W alloy) were similar to those obtained on the crystalline alloys and no correlation between amorphousity and enhanced passivity was found. Figure 8 compares two representative Al-W curves (both crystalline alloys) with our earlier results for Al-8%Mo alloys. This figure reveals that the addition of 10.3%W to aluminum can increase the breakdown potential by as much as 2600 mV. This represents a significant improvement over the breakdown potentials that we observed earlier for Al-Ta, Al-Cr, and Al-Mo alloys.

Potentiodynamic polarization was also carried out on duplicate specimens taken from the films produced using the binary Al-1%W targets (see Fig. 9). These specimens exhibited open circuit potentials 300 mV lower than those observed for the cosputter-deposited alloys. We attribute this difference in E_{oc} to the lower W concentrations in these alloys. Unlike the alloys containing higher W concentrations, the amount of W in this alloy is too low to significantly catalyze the reduction reaction and thereby increase the open circuit potential. The specimens exhibited low passive current densities that were independent of potential in the passive region. Pitting potentials of -178 and -44 mV were obtained for the two specimens. Although these values are significantly lower than those observed for the higher W concentrations, they still represent a dramatic improvement over unalloyed aluminum.

Anodic potentiodynamic polarization scans were generated on Al-8%W alloys heat treated for 1 hour at 400°C to determine the effect of precipitates on localized corrosion resistance. The results of these experiments are presented in Fig. 10. Although the presence of precipitates in the alloy clearly degrades the localized corrosion resistance of the Al-W alloys, the performance of these specimens is still equivalent to that of the nonheat-treated Al-8%Mo alloys. Of all the alloys evaluated to date, only Al-Ta and Al-W alloys exhibited some degree of corrosion resistance after heat treatment. One possi-

ble explanation is that the potential difference between the precipitates and the matrix for these alloys does not promote the formulation of local galvanic cells. However, the potential differences between the intermetallics and the matrix is not known. Longer heat treatments (up to 24 hours) at the same temperature are planned for the coming year so that we may assess the effect of reduced W in solid solution on passivity.

RAE alloy 72

The polarization behavior of RAE 72 in aerated 0.1 M KCl is presented in Fig. 11 . The alloy exhibited an open circuit potential of approximately -800 mV and a passive current density of approximately 0.5 $\mu A/cm^2$. The observed breakdown potentials varied from -499 to -216 mV. Because of the lack of agreement for E_p in replicate samples, the electrochemical scratch technique was employed to determine the critical potential for breakdown. Duplicate specimens were tested using a scratch voltage of 1 V and potential steps of 50 or 25 mV. These tests revealed that the protection potential was between -475 and -500 mV. Following testing, a uniform dispersion of very fine pits was observed on the specimen surfaces. The morphology of attack leads us to believe that the iron precipitates act as nucleation sites for pitting. Despite the rather narrow passive region obtained for these ternary specimens, the technique shows a great deal of promise for producing binary alloys in which several atomic percent of the solute can be retained in solid solution. In the coming year, we will be evaluating an Al-Cr binary alloy in which all of the Cr (5-6%) is retained in solid solution.

3.4 Surface Analysis

XPS analysis of the as-deposited Al-W specimens showed that the oxide film was Al_2O_3 and that no oxidized solute was present in the film. The description also applies to all other alloys investigated to date. Because the film is thin (~4 nm), the metallic region near the interface is also probed by XPS. It shows two metallic states, which we attribute to elemental and alloyed components. A similar pair of states was also observed for Al-Mo and Al-Cr alloys (2,4). Presumably, the elemental component forms when the Al is preferentially oxidized and the metallic solute is concentrated at the interface. We previously showed this occurred for Al-Mo and Al-Cr alloys

and will investigate further whether Al dealloys from the W for Al-W alloys in the upcoming year.

When the specimen is immersed into the solution and allowed to come to E_{oc}, the film thickens very slightly (~4.5 nm) and hydrates so that AlOOH is the dominant constituent. Unlike Al-Mo, Al-Cr, Al-Ta, and Al-Zr alloys, no oxidized solute is detectable in the film at the open circuit potential. This is also true for the first polarization step of the series (+500 mV vs E_{oc}), but at higher potentials (+ 800 mV vs E_{oc}) and above up to E_p, WO_3 (or a WO_4^{-2} species, we cannot distinguish between them) forms in the passive film. However, the WO_3 remains a small component of the oxide (<1 mol.%). Throughout the polarization sequence, the passive film remains thin (≤6 nm). Such a thin film was also observed for the Al-Ta, but in that case the solute continued to oxidize until it was comparable in concentration to oxidized Al. For all other alloy systems we have investigated, the film thickened during polarization until the metallic substrate could no longer be detected with XPS.

The similarity in minimal growth of the passive films of Al-W and Al-Ta is interesting, considering that these are the best alloys we have yet investigated. In the upcoming year, we will repeat these experiments with high and low concentration Al-W alloys, as well as with crystalline and amorphous specimens. From these results, we hope to identify the mechanisms responsible for the superior corrosion resistance of these alloys.

4.0 DISCUSSION

Of the alloys examined to date, the Al-W alloys exhibit the best resistance to localized corrosion. Figure 12 compares the polarization behavior for an Al-1.5%W alloy, an Al-8.5%W alloy and an Al-10.3%W alloy with the polarization behavior for all of the previously examined alloys. The localized corrosion resistance of the Al-1.5%W alloy is comparable to that observed for the Al-Cr alloys with chromium concentrations between 4 and 8%. The addition of just 1.5%W to Al increases the pitting potential over 500 mV and significantly enhances the localized corrosion resistance of Al beyond any commercially available alloy. The addition of 8.5%W results in dramatic improvements in E_p with respect to the Al-8%Ta and Al-8%Mo alloys. Additionally, heat-treated Al-8%W alloys that contain precipitates exhibit localized corrosion performance comparable to as-deposited, precipitate-free Al-8%Ta and Al-8%Mo alloys. At an even higher W concentration of 10.3%, the shift in E_p to a value slightly less than 2000 mV is even more dramatic.

Irrespective of the W concentration in the Al-W alloys, the passive current density remains essentially the same. Polarization behavior for replicate pure W specimens in aerated 0.1 M KCl (curves were produced under conditions identical to those used to produce our Al-W curves) are presented in Fig. 13. The pure W show no evidence of a breakdown potential in the potential region evaluated (E_{oc} to 2000 mV). However, pure W does exhibit a relatively high passive current density of approximately 100 $\mu A/cm^2$ in 0.1 M KCl (pH 7). This suggests that passivity is not enhanced as a result of the formation of a more chemically stable oxide. Indeed, surface analysis of the passive film reveals that initially no detectable oxidized solute is present in either the as-deposited film or the passive film polarized to potentials less than 165 mV. Instead, it seems likely that improved repassivation kinetics plays a major role in the enhanced passivity of Al-W alloys.

5.0 CONCLUSIONS

1. Super-saturated Al alloys containing several atomic percent of passivity enhancing elements such as Cr, Mo, Ta, and W can be produced by vapor deposition.

2. Room temperature storage of super-saturated, sputter-deposited Al-W, Al-V, and Al-Nb for 1 year does not result in the precipitation of a second phase. Similar results have been obtained previously for all of the other alloys with the exception of Al-Cu.

3. Of Al-Cr, Al-Mo and Al-Ta, only the Al-Ta alloys show a linear slope for E_p as a function of solute concentration. Thus, the Al-Ta system is a leading candidate for the production of a rapidly solidified powder for future dynamic compaction of a bulk alloy.

4. The addition of W to Al results in positive shifts in E_p of as much as 2600 mV. At low concentrations (~ 1.5 at.%), E_p for Al is shifted over 500 mV.

5. Al-8%W alloys heat treated for 1 hour at 100 C form a second phase. However, the localized corrosion resistance of these two-phase alloys is similar to that of the one-phase Al-Mo alloys.

6. High W concentrations (i.e,. >8.5 %) in solid solution with Al can lead to the formation of amorphous alloys.

7. Physical vapor deposition appears to be a promising method for the production of bulk Al alloys that retain several atomic percent of passivity-enhancing solutes in solid solution.

Future Work

1. Determine the passivity behavior of ternary Al-Ta-W alloys.

2. Further investigate the mechanisms of passivity of Al-W and Al Ta-W alloys (if promising).

3. Have A-W and Al-Ta powders produced and dynamically compacted. Characterize the alloys and evaluate their passivity behavior.

4. Evaluate the passivity behavior of a RAE vapor-deposited Al-Cr alloy and pursue feasibility and availability of vapor-deposited Al-W or Al-Ta alloys.

Acknowledgements

We gratefully acknowledge the assistance of J.G. Slunt in the preparation of the sputter deposited films and K.A. Olver for conducting the X-ray photoelectron spectroscopy. We would like to thank R.W. Gardiner of the Royal Aerospace Establishment for donating the RAE Alloy 72 used in this investigation. Additionally, we would like to thank G. S. Frankel and M.A Russak of the IBM Research Division - T.J. Watson Research Center for their helpful discussions concerning highly alloyed Al thin films.

6.0 REFERENCES

1. W.C. Moshier, G.D. Davis, J.S. Ahearn, and H.F. Hough, MML TR 86 79c, Martin Marietta Laboratories, Baltimore, MD, September 1986.

2. W.C. Moshier, G.D. Davis, J.S. Ahearn, and H.F. Hough, J. Electrochem. Soc. **134**, 2677 (1987).

3. W.C. Moshier, G.D. Davis, G.O. Cote, H.F. Hough and M.E. Vogelsang, MML TR 87-75c, Martin Marietta Laboratories, Baltimore, MD, September 1987.

4. W.C. Moshier, G.D. Davis, and G.O. Cote, J. Electrochem. Soc. **136**, 356 (1989).

5. G.D. Davis, W.C. Moshier, T.L. Fritz ,G.O. Cote, G. G. Long and D.R. Black MML TR 89-12c, Martin Marietta Laboratories, Baltimore, MD January 1989.

6. G.D. Davis, W.C. Moshier, T.L. Fritz, and G.O. Cote, J. Electrochemical Society, **137**, 422 (1990).

7. J. Tousek, *Theoretical Aspects of the Localized Corrosion of Metals* (Trans Tech Publications, Switzerland, 1985), p. 139.

8. N. Bui, A. Irhzo, F. Dabosi, and Y. Limouzin-Maire, Corrosion **39**, 491 (1983).

9. B.A. Shaw, T.L. Fritz, G.D. Davis, and W.C. Moshier, accepted for publication in J. Electrochem. Society.

10. R.W. Gardiner and M.C. McConnell, Metals Matl. **3**, 254 (1987).

11. R.L. Bickerdike, D. Clark, J.N. Eastabrook, G. Hughes, W.N. Mair, P.G. Partridge and H.C. Ranson, Int. J. Rapid Solidification, **2**, 1 (1986).

12. M.C. McConnell and P.G. Partridge, Acta Metall. **35**, 1973 (1987).

13. M. Nathan, Mater. Lett. **3**, 319 (1985).

14. ASTM Standard Test Method for Pitting or Crevice Corrosion of Metallic Surgical Implant Materials, F 746-87, (ASTM, Philadelphia, PA, 1987), p. 81.

15. B.C. Syrett, Corrosion **33**, 221 (1977).

16. D.A. Aylor and P.J. Moran, J. Electrochem. Soc. **133**, 868 (1986).

17. W.C. Moshier, G.D. Davis and J.S. Ahearn, Corros. Sci. **27**, 785 (1987).

18. G.D. Davis, W.C. Moshier, J.S. Ahearn, H.F. Hough and G.O. Cote, J. Vac. Sci. Technol., **A 5** 1152 (1987).

19. ASTM Standard Method of Salt Spray (Fog) Testing, B117-85, ASTM Annual Book of Standards (ASTM, Philadelphia, PA, 1987), p. 34.

20. Private communication with J. Frankel (IBM Research Division - T. J. Watson Research Center).

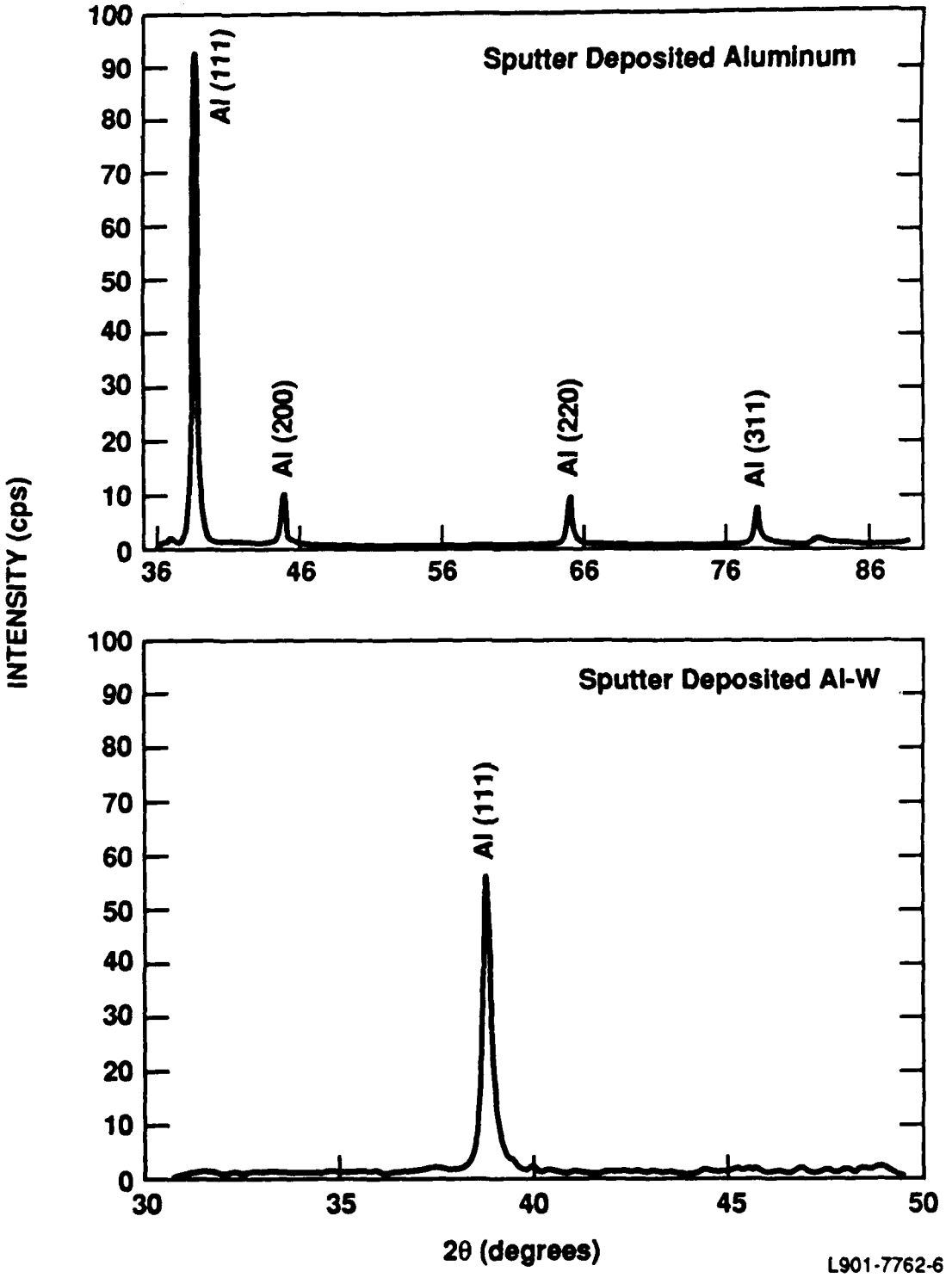

Figure 1. Glancing angle X-ray diffraction pattern for sputter-deposited Al, and a cosputter-deposited Al-86%W alloy (glancing angle of 10°).

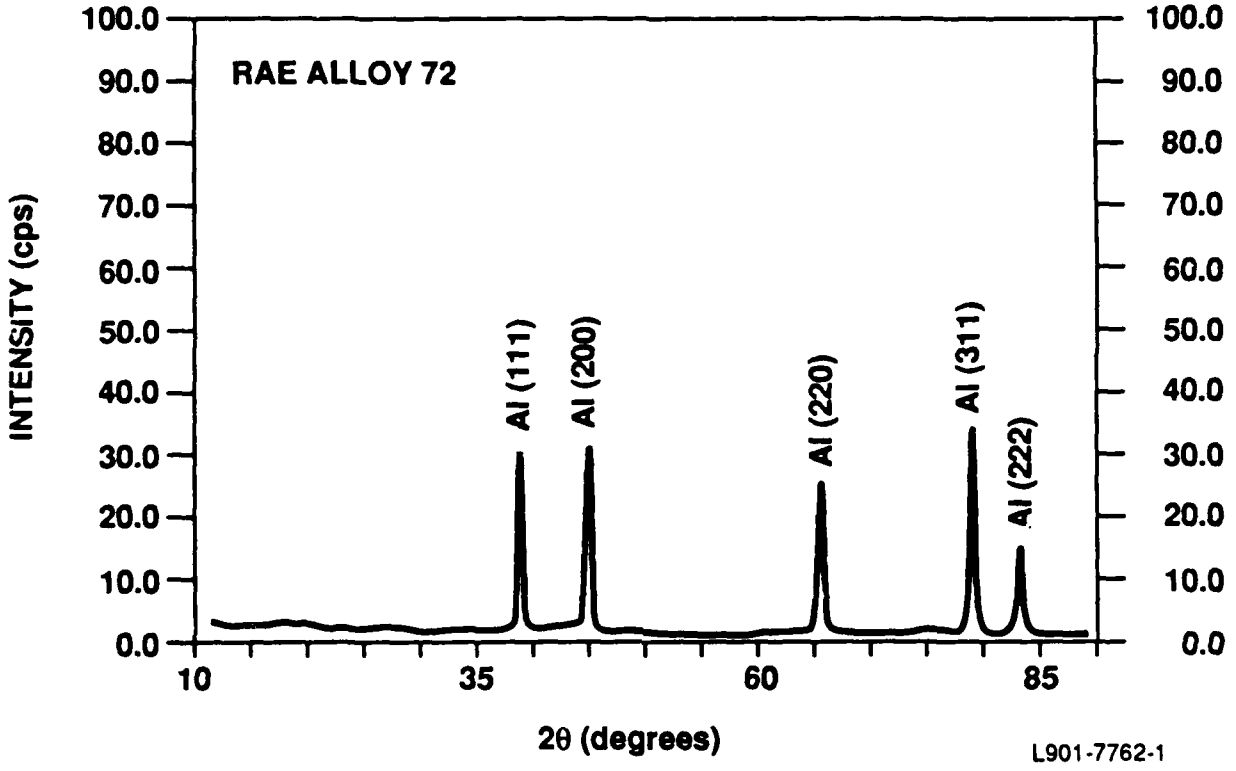

Figure 2. Glancing angle X-ray diffraction pattern for Al-Cr-Fe (RAE alloy 72) (glancing angle of 10°).

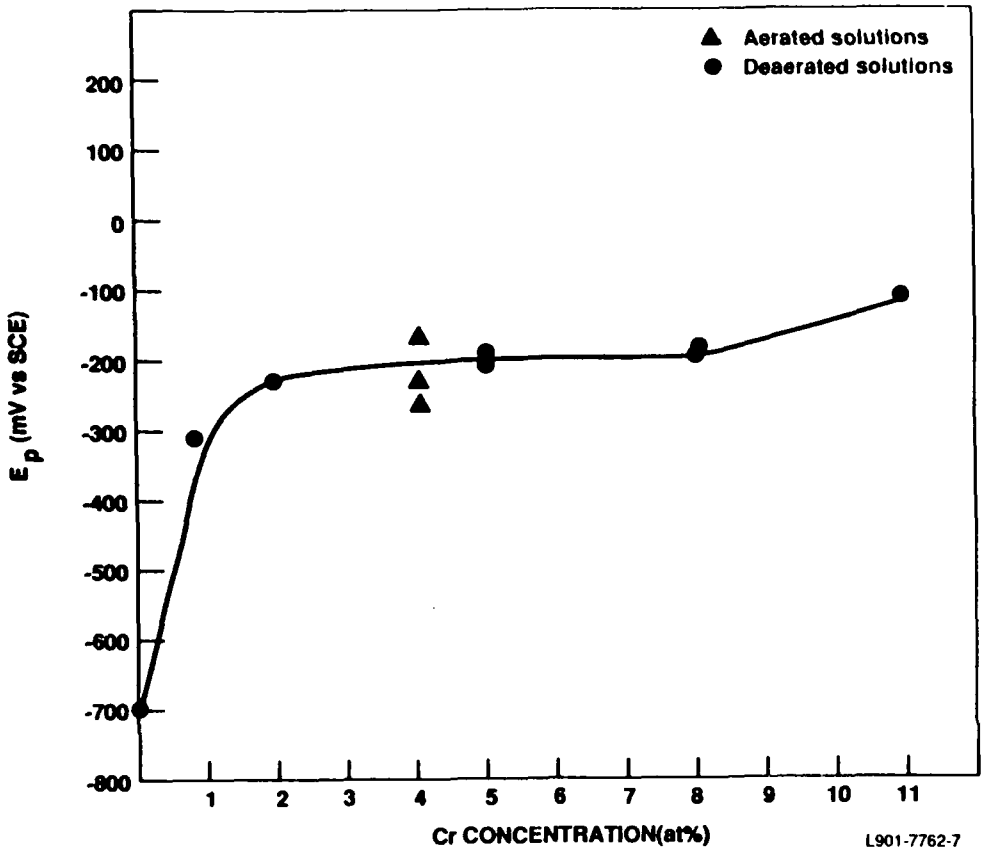

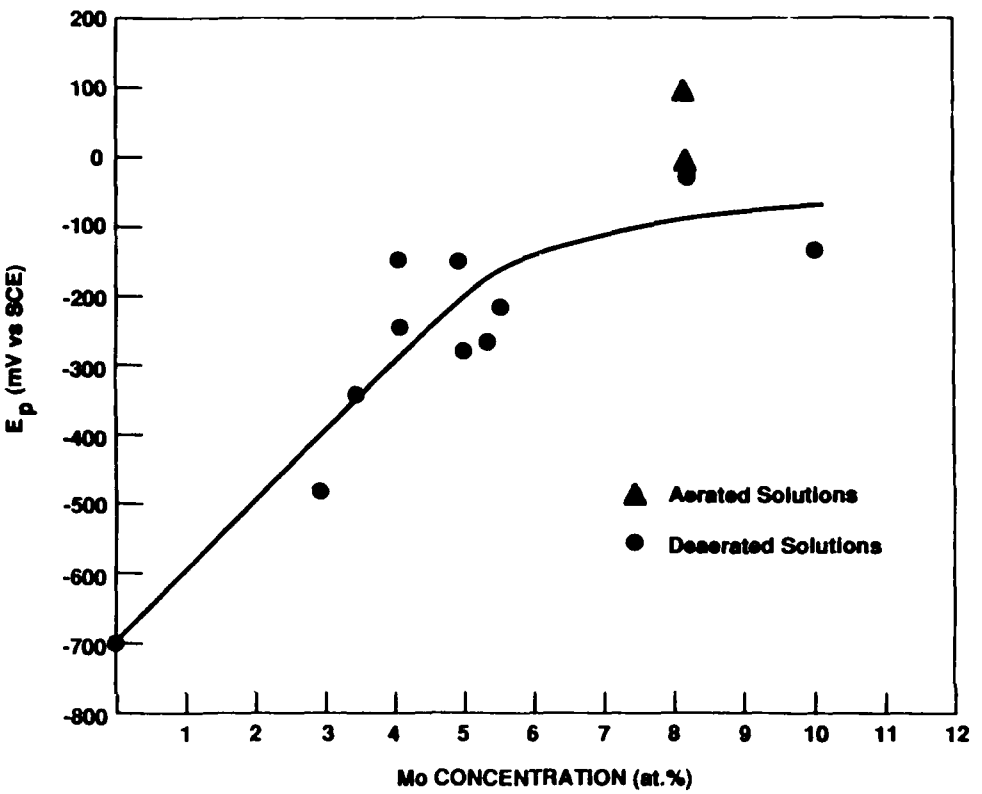

Figure 3. Pitting potential (E_p) vs solute concentration data for a) Al-Cr alloys and b) Al-Mo alloys.

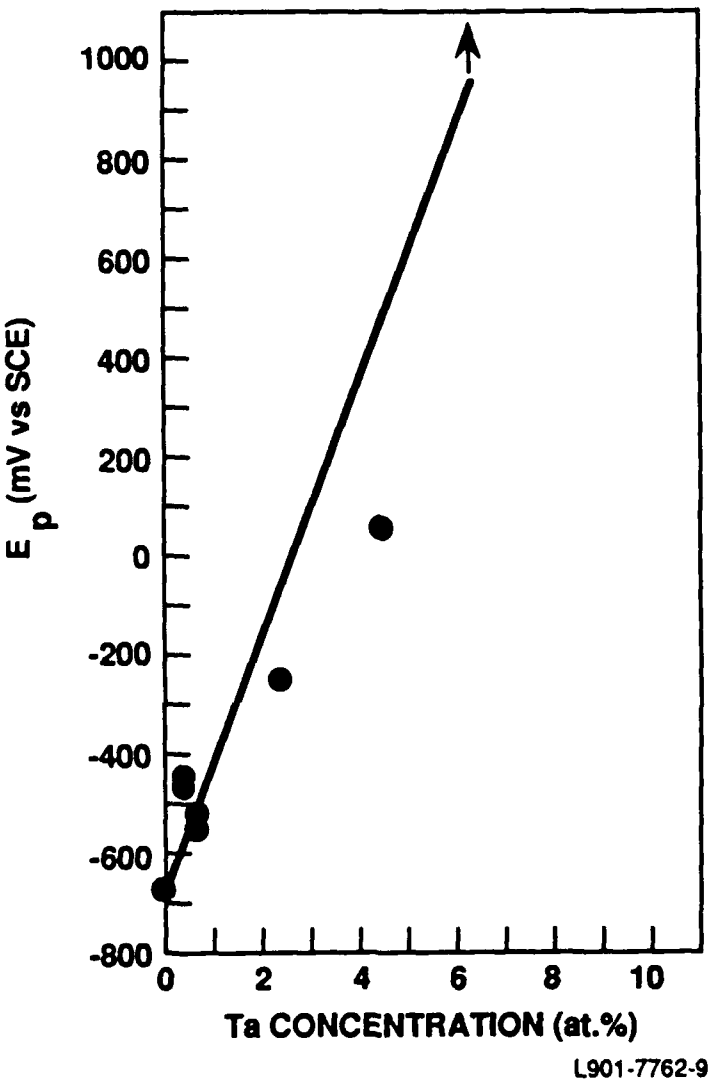

Figure 4. Pitting potential (E_p) solute concentration for Al-Ta alloys.

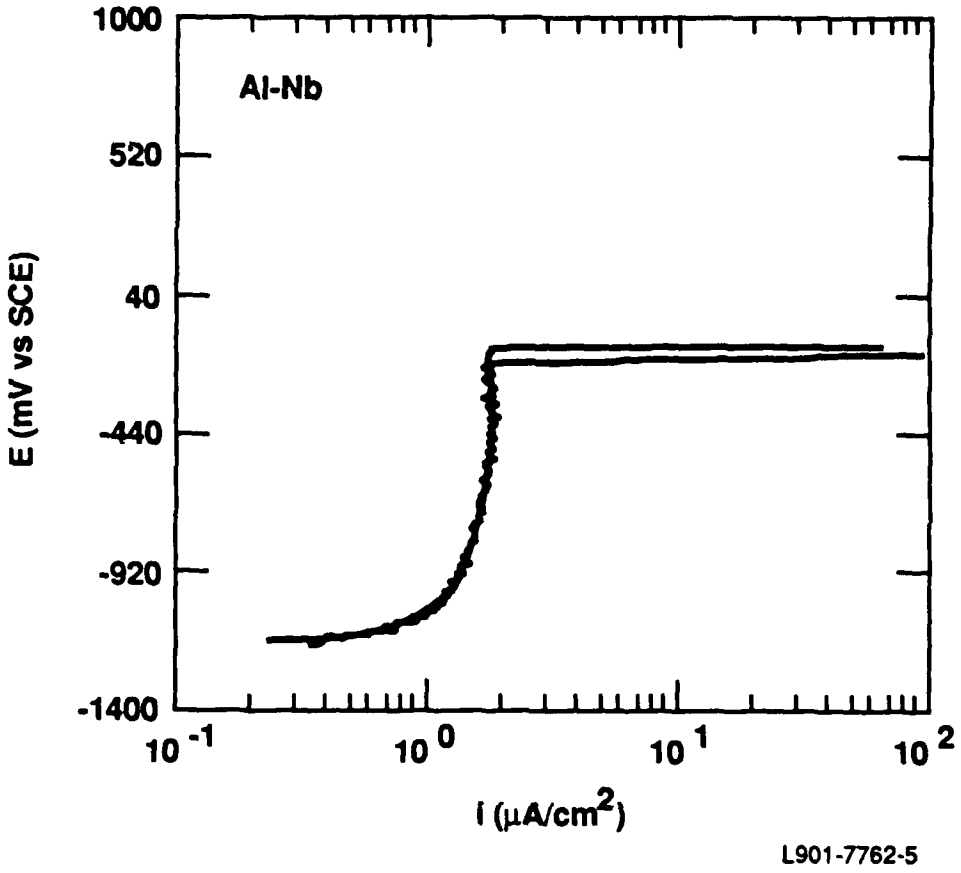

Figure 5. Anodic polarization behavior of duplicate Al-Nb specimens (4.5 - 5.5at.%Nb).

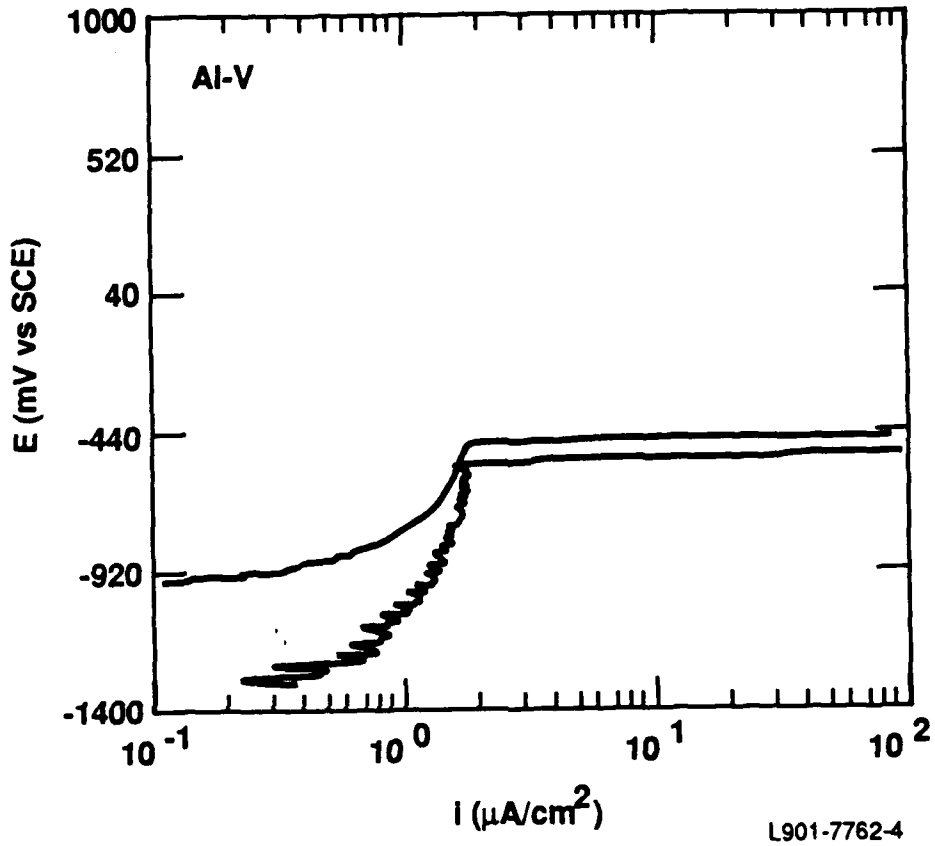

Figure 6. Anodic polarization behavior of duplicate Al-V specimens (0.7 - 2.6at.%V).

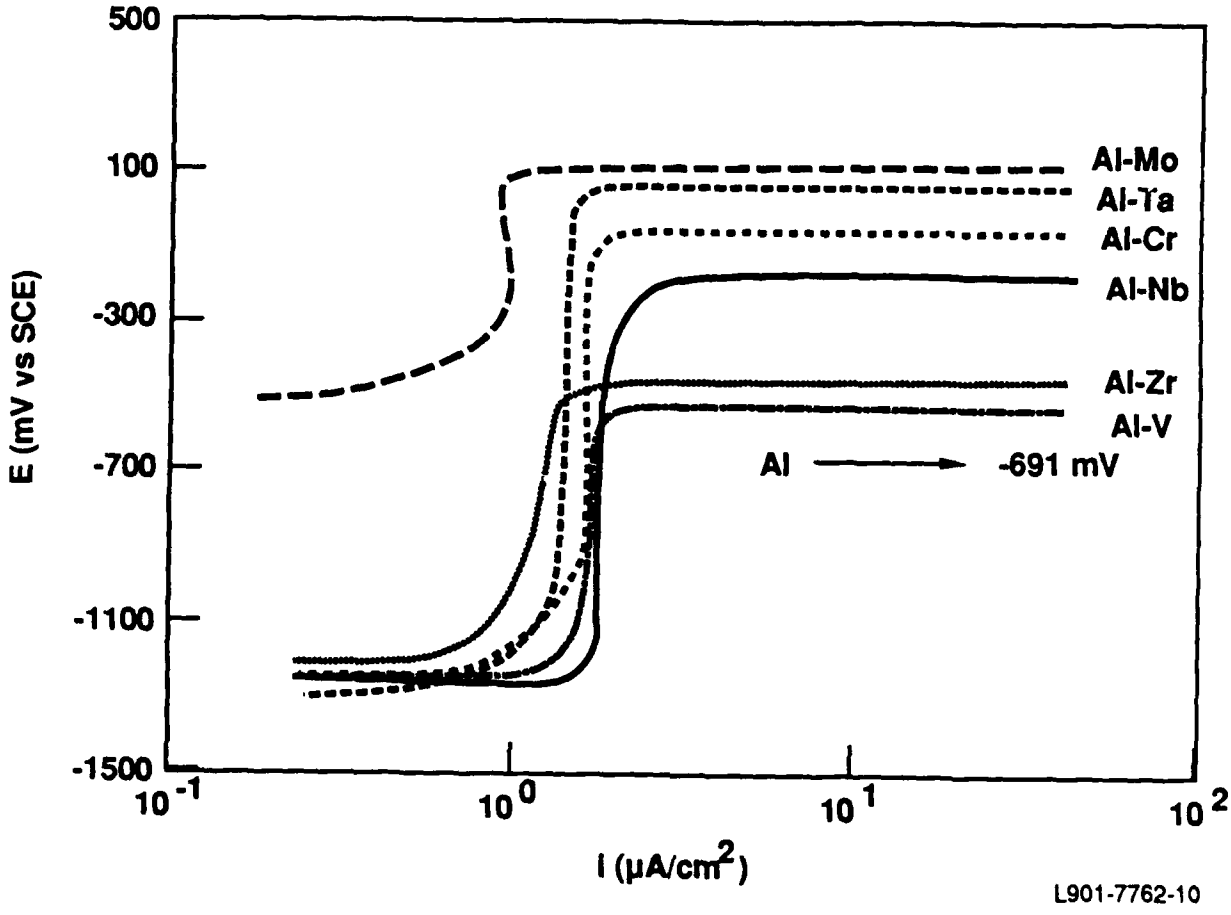

Figure 7. Anodic polarization behavior of Al-Nb and Al-V compared with Al-8%Mo, Al-8%Ta, Al-4%Cr, Al-3%Zr and pure Al.

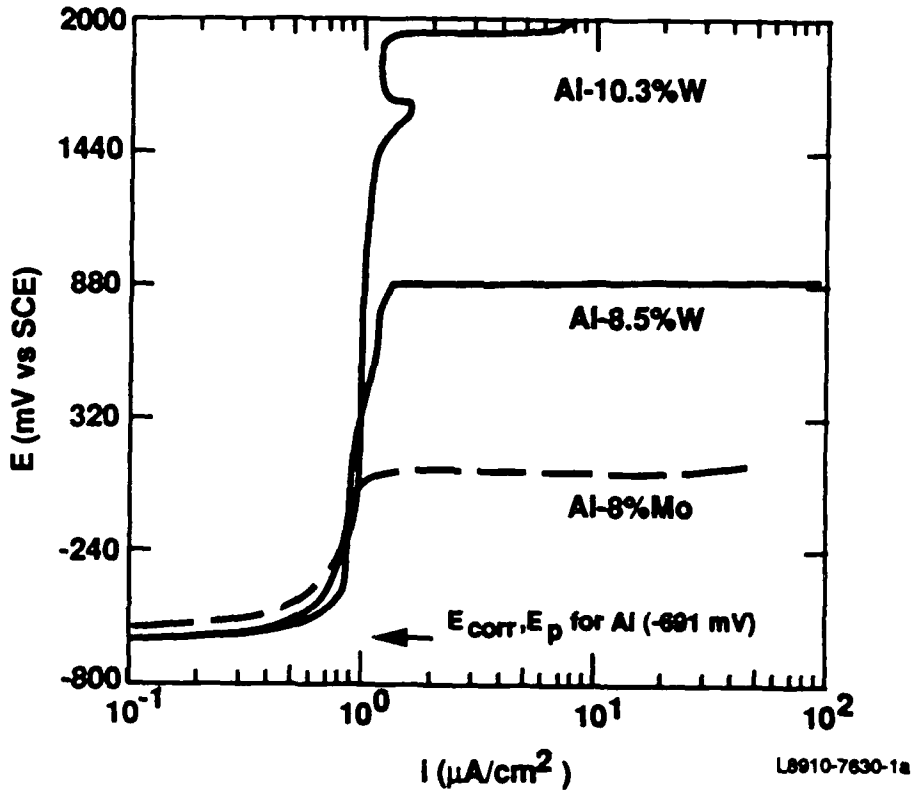

Figure 8. Anodic polarization behavior of Al-W alloys compared with Al-8%Mo and pure aluminum.

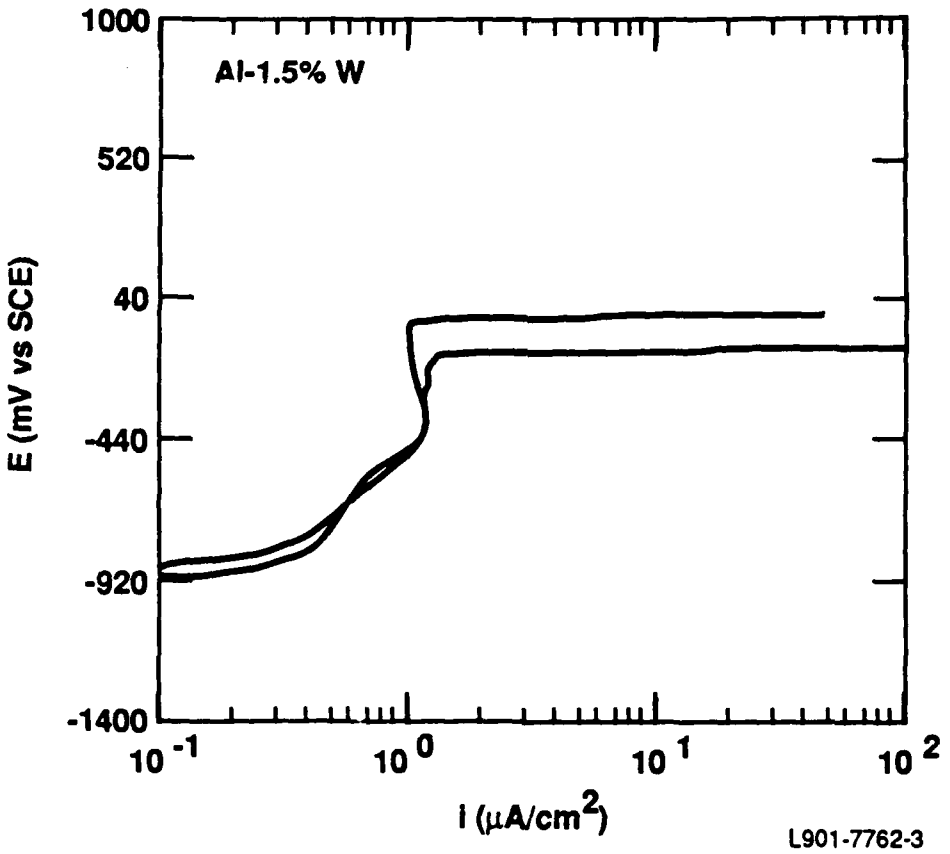

Figure 9. Anodic polarization behavior for duplicate Al-1.5%W alloys.

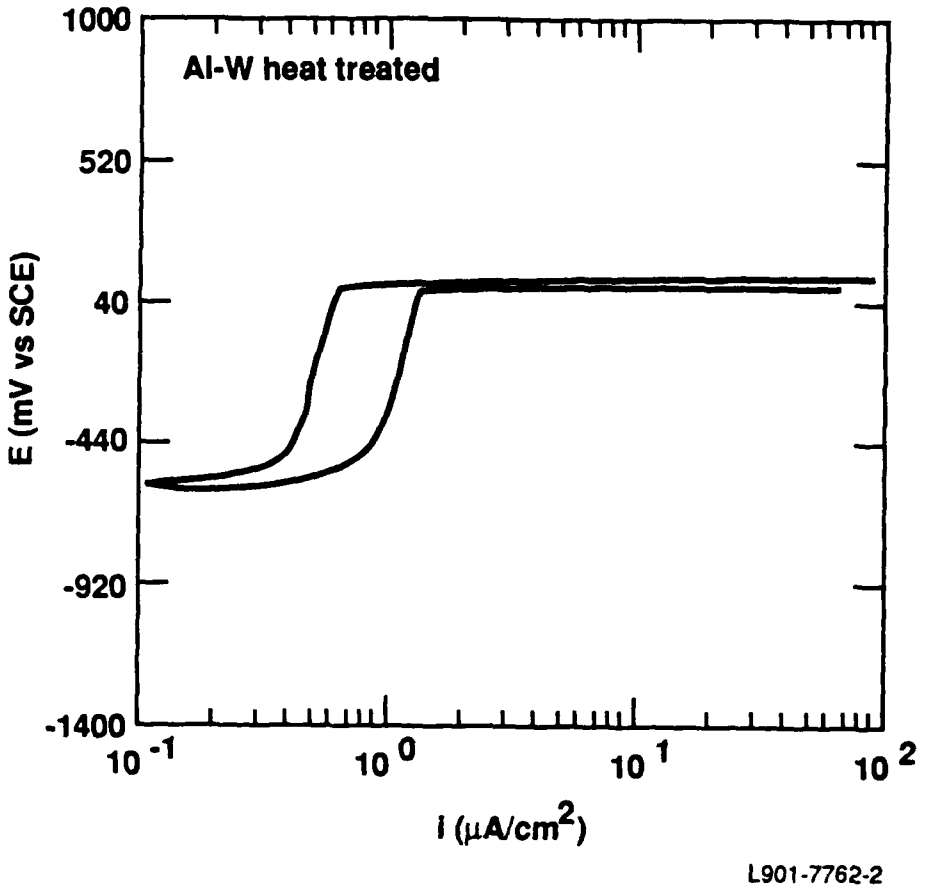

Figure 10. Anodic polarization behavior for duplicate AL-8%W alloys heat treated for 1 hour at 400°C.

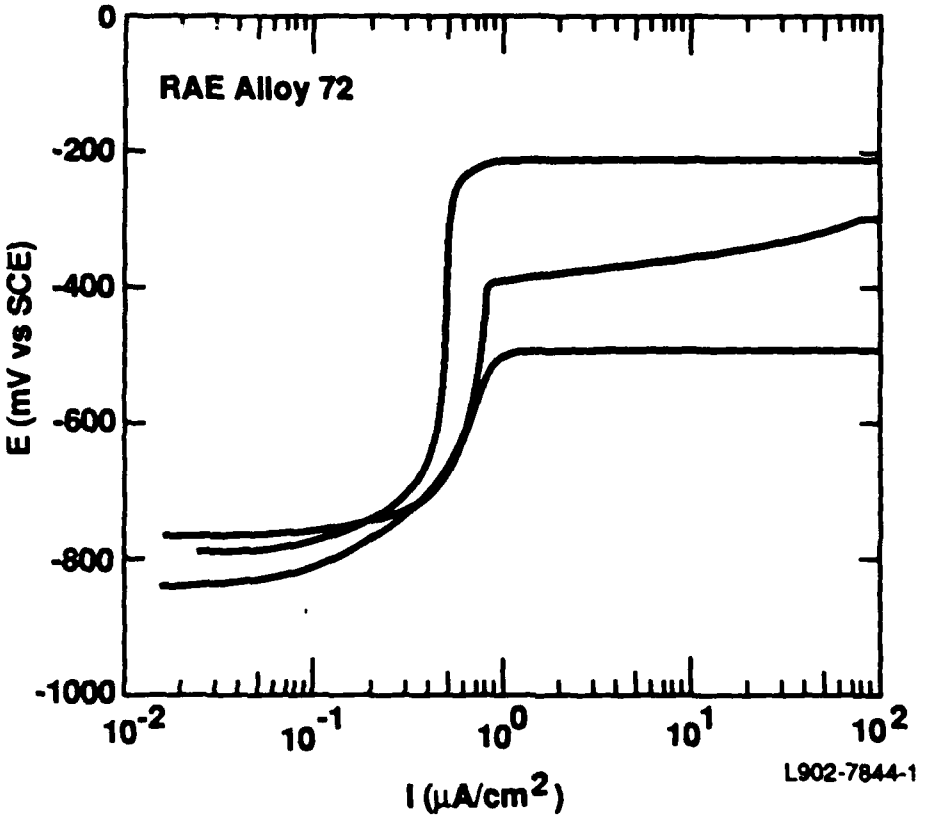

Figure 11. Anodic polarization behavior for RAE alloy 72.

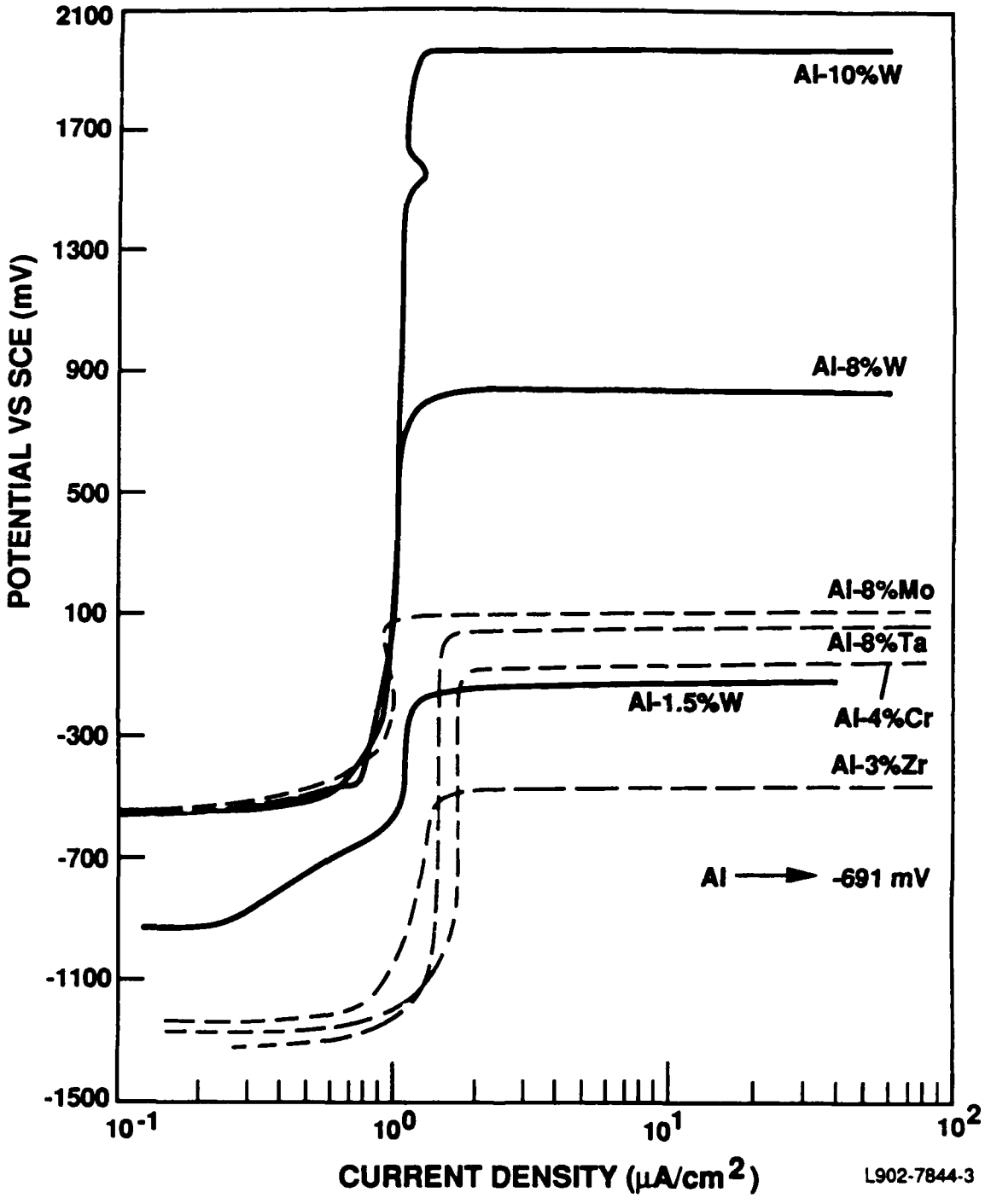

Figure 12. Anodic polarization behavior of Al-W alloys compared with previously reported data.

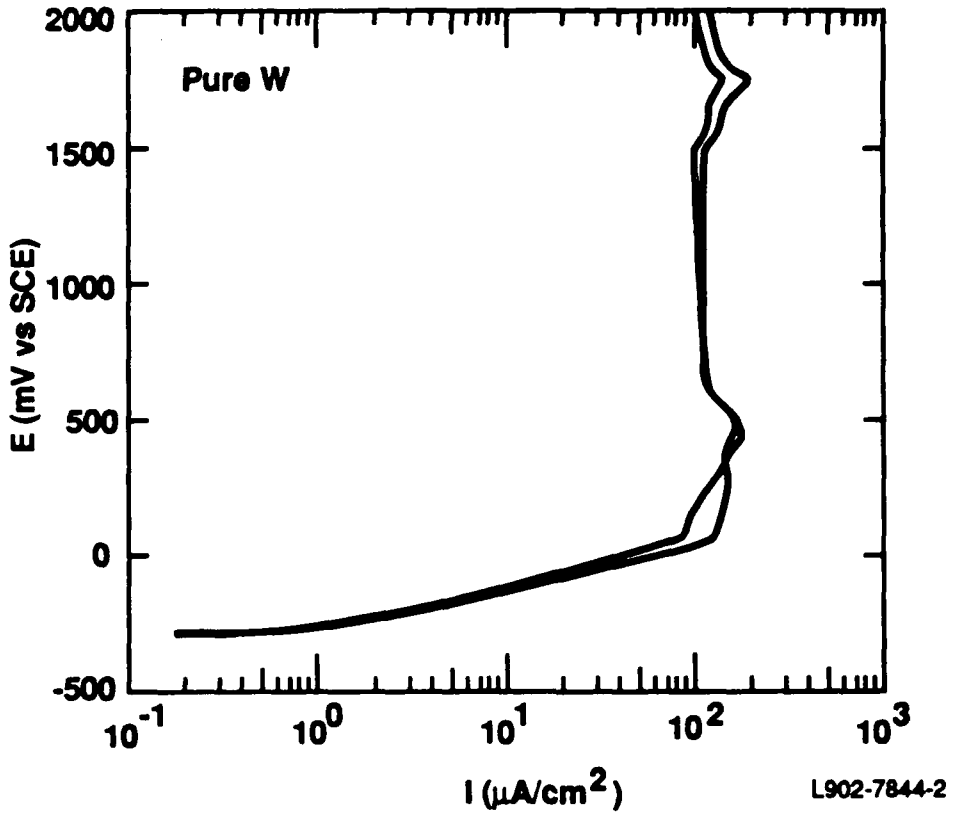

Figure 13. Anodic polarization behavior for duplicate pure W specimens.